JOURNAL OF Materials CHEMISTRY

Cyanine induced aggregation in *meso*-tetrakis(4-sulfonatophenyl)porphyrin anions

A. S. R. Koti and N. Periasamy*

Department of Chemical Sciences, Tata Institute of Fundamental Research, Homi Bhabha Road, Colaba, Mumbai, 400 005, India. Fax: 091 22 215 2110; E-mail: peri@tifr.res.in

Received 22nd February 2002, Accepted 15th April 2002
First published as an Advance Article on the web 20th May 2002

The interaction of anionic *meso*-tetrakis(4-sulfonatophenyl)porphyrin (H_4TPPS^{2-} and H_2TPPS^{4-}) with cationic cyanines, $DiOC_2(3)$ and $DiOC_6(3)$ were studied. The cyanine with the hexyl chain, $DiOC_6(3)$ induced aggregation of the porphyrin with new absorption and emission bands. The stoichiometric ratio of porphyrin : cyanine in the aggregate is $\sim$1 : 4. UV–Vis absorption, fluorescence, fluorescence lifetime, resonance light scattering and dynamic light scattering studies were used for further characterization of the aggregate. The spectroscopic aggregation number for the porphyrin in the aggregate was estimated to be $\sim$2.5 by comparing the half width of its emission spectrum with that of the monomer. The spontaneous aggregation of porphyrin with $DiOC_6(3)$, but not with $DiOC_2(3)$, indicates the role of the chain length of the alkyl group attached to the benzoxazole in the cyanine dye for stabilizing the structure of the aggregate.

I. Introduction

Self-assembled molecular aggregates formed by non-covalent interactions are important materials for molecular devices, as models of biomimetic systems and for supramolecular synthesis.[1,2] In recent years, much interest has been focused on J- and H-aggregates in which the molecular arrangement is highly ordered.[3] In J-aggregates, the one dimensional strongly coupled molecular arrangement is end-to-end (side by side) and the first independent observation was in 1,1′-diethyl-2,2′-cyanine chloride by Jelly[4] and Scheibe.[5] On the other hand in H-aggregates, the one dimensional strongly coupled molecular arrangement is face-to-face. Exciton theory[6] predicts a red shift of absorption in the case of J-aggregates[7,8] and a blue shift of absorption in the case of H-aggregates.[9,10]

Two important classes of compounds, which form J- and H-aggregates, are water-soluble porphyrins and cyanine dyes. The porphyrin, *meso*-tetrakis(4-sulfonatophenyl)porphine (H_2TPPS^{4-}) is known to form J-aggregates in acidic conditions[11] or at very high ionic strength[12–14] which has been confirmed by resonance light scattering,[15] circular dichroism and polarization,[16] fluorescence lifetime and anisotropy,[12] and dynamic light scattering.[17] Recently it has been shown that the porphyrin H_2TPPS^{4-} forms both J- and H-aggregates with the cationic surfactant cetyltrimethylammonium bromide (CTAB) with stoichiometric ratios of porphyrin : surfactant at 1 : 2 and 1 : 4 respectively.[14] Cyanine dyes are intensely coloured compounds and a typical structure consists of two heteroaromatic fragments linked by a polymethine chain. The photophysical properties of cyanine dyes are readily tuned by varying the heterocyclic moieties and polymethine bridge length. Cyanines have been used extensively as photosensitizers in photography[18] and as fluorescent probes for biomembrane fluidity[19–21] and potential.[22,23] The aggregation of ionic cyanines on helical nucleic acids,[24–26] peptides[27] and lipid assemblies[28] has also been demonstrated. Formation of heteroaggregates between anionic and cationic porphyrins has also been reported.[29]

In this paper we report detailed spectroscopic studies on porphyrin–cyanine interactions. The porphyrin is *meso*-tetrakis(4-sulfonatophenyl)porphine (H_2TPPS^{4-}) and the two cyanine dyes 3,3′-diethyloxacarbocyanine iodide {2-[3-(3-ethyl-2,3-dihydrobenzoxazolylidene)propenyl]-3-ethylbenzoxazolium iodide} ($DiOC_2(3)$) and 3,3′-dihexyloxacarbocyanine iodide {2-[3-(3-hexyl-2,3-dihydrobenzoxazolylidene)propenyl]-3-hexylbenzoxazolium iodide} ($DiOC_6(3)$) are symmetrical cationic cyanine dyes consisting of two *N*-ethyl and *N*-hexyl substituted benzoxazole groups linked by a trimethine bridge, respectively. Cyanine induced aggregation of the porphyrin anions and the role of alkyl chain length on the aggregation are discussed.

II. Materials and methods

The cyanine dyes 3,3′-diethyloxacarbocyanine iodide ($DiOC_2(3)$) and 3,3′-dihexyloxacarbocyanine iodide ($DiOC_6(3)$) were purchased from Aldrich Chemicals (USA), and the sodium salt of *meso*-tetrakis(4-sulfonatophenyl)porphyrin (H_2TPPS^{4-}) was purchased from Strem Chemicals (USA). The structures are shown in Fig. 1. The purity of all three dyes was tested by thin-layer chromatography. Methanol (spectroscopy grade, S. D. Fine-Chemicals, Mumbai, India) was used as a solvent for making cyanine stock solutions. The porphyrin stock solution was made in deionized water. Molar extinction coefficients used for calculating the concentration of the cyanines[30] are 153 000 M^{-1} cm^{-1} at 482 nm for $DiOC_2(3)$ and 154 000 M^{-1} cm^{-1} at 484 nm for $DiOC_6(3)$ in methanol. For the measurement of the concentration of porphyrin[31] H_2TPPS^{4-} we used 442 000 M^{-1} cm^{-1} at 434 nm at pH 3. In stoichiometric studies 500 000 M^{-1} cm^{-1} at 414 nm in methanol was taken as the molar extinction coefficient for H_2TPPS^{4-}. Absorption studies were done on a Shimazdu spectrophotometer. Steady state fluorescence spectra, quantum yield measurements and resonance light scattering spectra were recorded using a spectrofluorimeter (Fluorolog FL111 T-format spectrometer) and corrected for the spectral sensitivity of the photomultiplier (Hamamatsu R928A). The quantum yield of H_4TPPS^{2-} is taken as 1.0 and all other quantum yield values are relative to this value using the area of the emission spectra and absorbances at the respective excitation wavelength. Dynamic light scattering experiments were done using a set up that uses a laser (826.8 nm, 55 mW) and an avalanche photodiode detector (APD) detector. Time resolved fluorescence decays were obtained by time correlated single photon counting (TCSPC) method and the data were fitted to a multi-exponential function.[32] The sample was excited

 DOI: 10.1039/b201914k

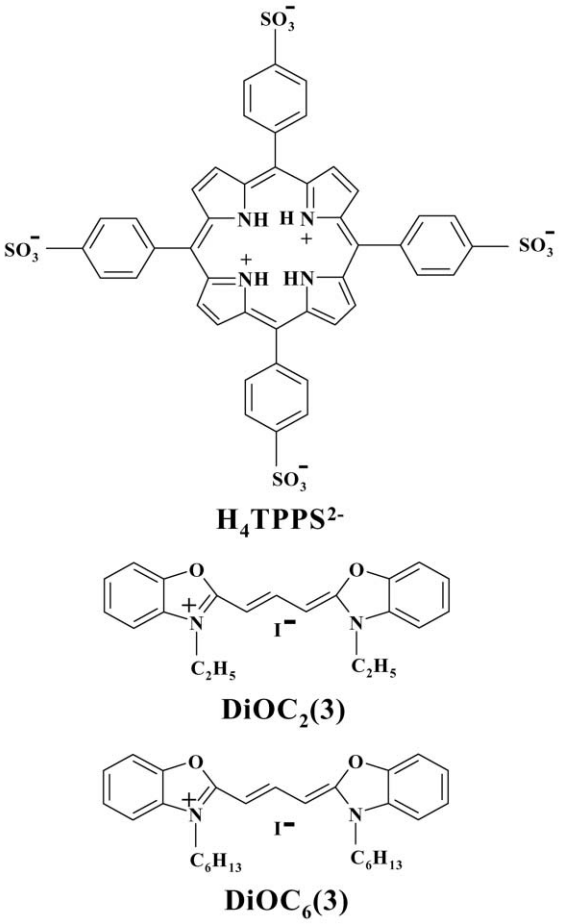

Fig. 1 Structures of the dianion of tetrakis(4-sulfonatophenyl)porphine (H_4TPPS^{2-}), 3,3′-diethyloxacarbocyanine iodide ($DiOC_2(3)$) and 3,3′-dihexyloxacarbocyanine iodide ($DiOC_6(3)$).

by 'vertically' polarized picosecond laser pulses (pulse width $\sim$ 2 ps) from a high repetition rate (4 MHz) derived from a tunable, mode-locked Ti-sapphire laser, pulse picker and frequency doubler. The wavelength of excitation was chosen as 462 nm for all time resolved fluorescence studies. Fluorescence emission at the magic angle (54.7°) was dispersed in a monochromator (*f*/4, spectral width 2.5 nm) and counted ($4–5 \times 10^3\ s^{-1}$) by a MCP PMT (R2809), and processed through constant fraction discriminator (CFD), time-to-amplitude convertor (TAC) and multichannel analyzer (MCA). Fluorescence decays were collected at the interval of 20 ps/channel. The instrument response function is $\sim$40 ps.

All the measurements were carried out in an air-saturated solution and at room temperature (25 ± 1 °C). The buffers used for the experimental studies contained sodium acetate (10 mM) and sodium phosphate (10 mM) as the buffering agents.

III. Results

Absorption studies

The pK_a of the *meso*-tetrakis(4-sulfonatophenyl)porphyrin ($H_2TPPS^{4-} + 2H^+ \leftrightarrow H_4TPPS^{2-}$) is 4.8.[31] The tetraanion (H_2TPPS^{4-}) is stable above pH 6.0 and the absorption spectrum (not shown) consists of an intense Soret peak at 412 nm and four Q-band peaks at 515, 552, 580 and 633 nm. The porphyrin is a dianion below pH 3 and its absorption spectrum consists of a B band (Soret), which is intense and centered at 433 nm and two Q bands at 595 nm 644 nm (see Fig. 2). The spectral features of the tetraanion and dianion have been discussed in detail in previous studies.[12]

The effect of addition of the cyanine dye on the absorption

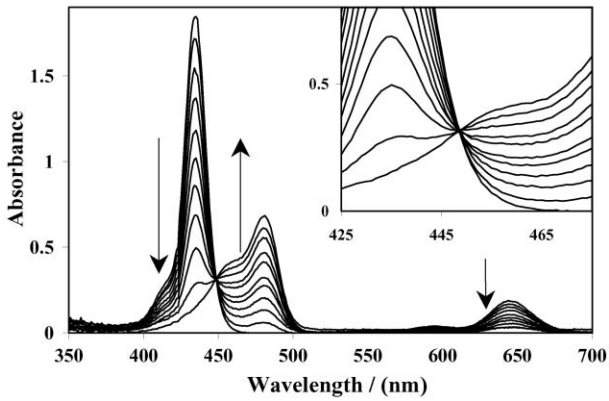

Fig. 2 UV–Vis analysis of H_4TPPS^{2-} interaction with $DiOC_2(3)$ in pH 3.0 buffer. Total concentration of H_4TPPS^{2-} and $DiOC_2(3)$ is 10 μM. The inset shows the region around the isosbestic point at 448 nm.

spectrum of the dianion (H_4TPPS^{2-}) and tetraanion (H_2TPPS^{4-}) was studied as follows. Absorption spectra were recorded for various ratios of porphyrin (H_4TPPS^{2-} or H_2TPPS^{4-}) : cyanine in a buffer of pH 3 or 7.4 while maintaining their total concentration at 10 μM. Two cyanines, $DiOC_2(3)$ and $DiOC_6(3)$, were used in this study. Fig. 2 and Fig. 3 show the absorption spectra for the interaction of dianion (H_4TPPS^{2-}) with $DiOC_2(3)$ and $DiOC_6(3)$, respectively. The spectra in Fig. 2 show an isosbestic point at 448 nm. This indicates that the absorption spectrum of the mixture (H_4TPPS^{2-} with $DiOC_2(3)$) is simply an addition of the spectra of the two components. This confirms that there is no interaction between H_4TPPS^{2-} and $DiOC_2(3)$. On the other hand, the spectra in Fig. 3 for the mixture (H_4TPPS^{2-} with $DiOC_6(3)$) does not show an isosbestic point. New absorption bands have appeared at 420 nm (instead of the original band at 433 nm) and in the 500–550 nm region, when the cyanine concentration is large. Neither the porphyrin dianion nor the cyanine dye absorbs in the region 500–550 nm. Similar studies of the interaction of the two cyanines with the tetraanion at pH 7.4 indicated that the tetraanion also forms new absorption bands only with $DiOC_6(3)$. Evidently, there is a strong interaction between H_4TPPS^{2-} or H_2TPPS^{4-} and the cyanine with hexyl chain ($DiOC_6(3)$) leading to the formation of new products.

The new product is not stable in solution, especially when the concentration of the porphyrin is high. Light scattering and other studies have shown that colloidal aggregates are formed and the product separates out slowly from the solution. Centrifugation of the sample is used for rapid separation of the colloidal particles. At very high concentration (>50 μM) of

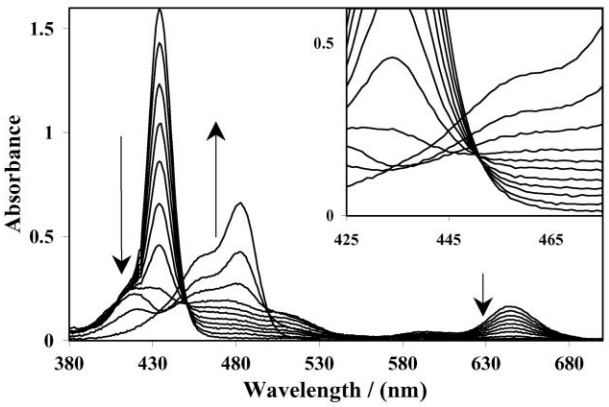

Fig. 3 UV–Vis analysis of H_4TPPS^{2-} interaction with $DiOC_6(3)$ in pH 3.0 buffer. Total concentration of H_4TPPS^{2-} and $DiOC_6(3)$ is 10 μM. The inset shows the absence of an isosbestic point near 450 nm.

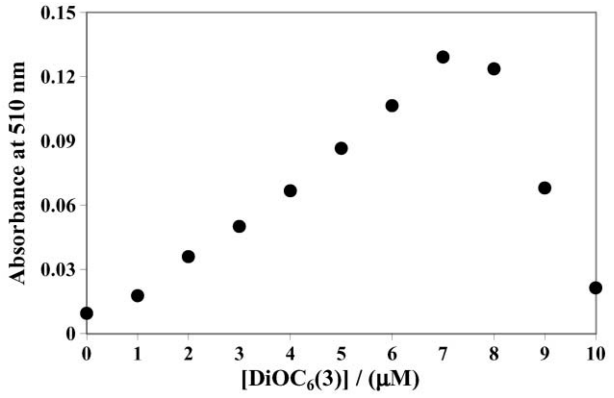

Fig. 4 Job plot constructed from mixing H_4TPPS^{2-} and $DiOC_6(3)$ together in variable ratios but constant total concentration (10 μM). Absorbance values at 510 nm are plotted versus the concentration of $DiOC_6(3)$.

H_4TPPS^{2-} and $DiOC_6(3)$ the solution becomes turbid and thin films are deposited on the walls of the container. The film of the aggregate of H_4TPPS^{2-} and $DiOC_6(3)$ is soluble in methanol but insoluble in non-polar solvents like carbon tetrachloride (CCl_4) and benzene (C_6H_6).

The stoichiometry at which the porphyrin–cyanine interaction gives maximum concentration of the new product is obtained from the Job plot of absorbance at 510 nm *vs.* the ratio of concentration of cyanine to porphyrin, which is shown in Fig. 4. The absorbance due to the product is a maximum for porphyrin : cyanine = 1 : 3.5. The stoichiometry of porphyrin : cyanine in the aggregate was also determined as follows. The solution of porphyrin (2 μM) and cyanine (8 μM) in the ratio of 1 : 4 (Fig. 4) was centrifuged at a speed of 10 000 rpm for 2 min and the aggregate was precipitated at the bottom. The solution containing the monomers of H_4TPPS^{2-} and $DiOC_6(3)$, if any, was removed. The aggregate was then dissolved in methanol. The aggregate is unstable in methanol and dissociates to individual components. The individual concentration of porphyrin and cyanine dye was determined from the absorbances at 414 nm and 484 nm, respectively. The stoichiometry of $[H_4TPPS^{2-}]$: $[DiOC_6(3)]$ in the aggregate was determined to be 1 : 4. The porphyrin–cyanine aggregate formed when the pH is 7.4 also had the same stoichiometric ratio.

Fluorescence studies

Fig. 5 shows the fluorescence spectrum (curve a) of the sample of H_4TPPS^{2-} (2 μM) and $DiOC_6(3)$ (8 μM) in buffer of pH 3. The fluorescence peaks are observed at 501 nm (cyanine) and 654 nm and 718 nm (porphyrin). The fluorescence spectra of the individual components are also shown. The fluorescence spectrum of $DiOC_6(3)$ alone has a band centered at 501 nm (curve b) and that of H_4TPPS^{2-} has a single band centered at 670 nm (curve c). The porphyrin peak is blue shifted by ~16 nm in the aggregate compared to the porphyrin dianion. It is seen that the dianion is practically absent in the sample either in free form or as a fluorescing component in the aggregate. It may also be noted here that the characteristic Soret band absorption of the dianion at 433 is absent in the absorption spectrum as well (Fig. 3).

The excitation spectrum of the aggregate for the emission at 654 nm is also shown in Fig. 5 (curve d). An excitation peak is observed at 420 nm (matching with the Soret peak seen in the absorption spectrum) and a broad band spanning from 450 nm to 550 nm. These features, peak positions and relative intensities, in the excitation spectrum are in one-to-one correspondence, qualitatively and quantitatively, with the features observed in the absorption spectrum of this sample. The important point here is that excitation in the region of 500–550 nm,

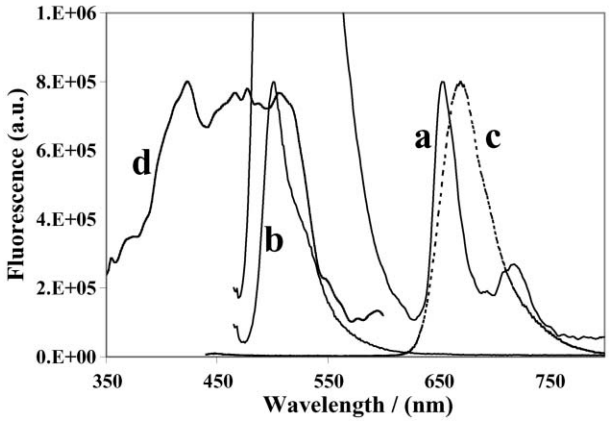

Fig. 5 Fluorescence spectra. (a) Fluorescence emission spectrum of the cyanine-aggregate of H_4TPPS^{2-} (5 μM) and $DiOC_6(3)$ (20 μM) at a concentration ratio of 1 : 4 (λ_{ex} = 444 nm). (b) Fluorescence spectrum of $DiOC_6(3)$ (5 μM) in pH 3.0 buffer. (c) Fluorescence spectrum of H_4TPPS^{2-} (5 μM) in pH 3.0 buffer. (d) Fluorescence excitation spectrum of the cyanine-aggregate of H_4TPPS^{2-} (5 μM) and $DiOC_6(3)$ (20 μM) at a concentration ratio of 1 : 4 (λ_{em} = 655 nm).

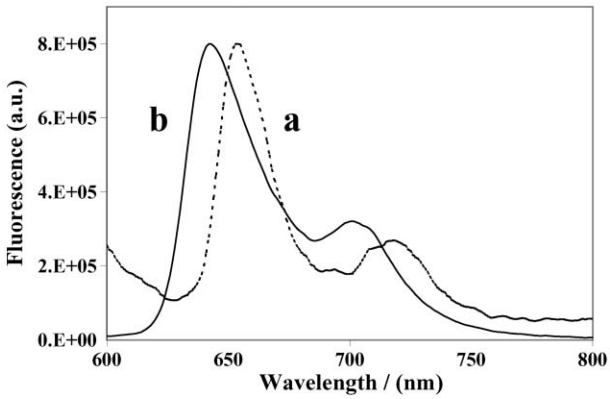

Fig. 6 Steady state fluorescence emission spectrum of (a) the cyanine-aggregate of H_4TPPS^{2-} (5 μM) and $DiOC_6(3)$ (20 μM); (b) the tetraanion H_2TPPS^{4-} (5 μM).

the region in which neither free porphyrin nor free cyanine absorbs, does give rise to porphyrin-like fluorescence emission at 654 nm and 718 nm.

In Fig. 6 we compare the fluorescence emission of the porphyrin–cyanine aggregate in buffer of pH 3 excited at 460 nm (curve a) with the emission spectrum of porphyrin tetraanion (H_2TPPS^{4-}) in buffer of pH 7.4 excited at 412 nm. The spectra are similar except for the red shift and a narrowing of the spectrum in the aggregate. Because of the similarity of the emission spectra, the emissive species in the aggregate is inferred to be the tetraanion-like porphyrin species. Similar fluorescence excitation and emission spectra were found with the porphyrin–cyanine aggregate prepared in pH 7.4 buffer.

In Table 1 we compare the quantum yield (ϕ) data for the above-mentioned porphyrin–cyanine aggregates prepared in pH 3.0 and pH 7.4 buffers. The measured quantum yields are relative to that of H_4TPPS^{2-}. The porphyrin–cyanine aggregates have values of 0.22 and 0.27 at pH 3.0 and pH 7.4 respectively.

Time resolved fluorescence studies

In order to understand further the nature of the aggregate formed in the interaction of porphyrin anion and $DiOC_6(3)$ in aqueous media at pH 3 and 7.4, time resolved fluorescence studies were carried out. The fluorescence lifetime of $DiOC_6(3)$ was measured to be ~100 ps. The fluorescence lifetime of free

Table 1 Time resolved fluorescence results; λ_{ex} is 462 nm

Sample	Quantum yield, ϕ^a	λ_{em}/nm	τ_1/ns	τ_2/ns	τ_3/ns	α_1	α_2	α_3	τ_{av}/ns	χ^2
In solution studies										
$DiOC_6(3)$	—	550	~0.10			1.0			~0.10	1.09
H_4TPPS^{2-}	1.0[c]	655	3.85			1.0			3.85	1.1
H_2TPPS^{4-}	0.71[d]	655	9.26			1.0			9.26	1.
Por[b]+cya (pH 3.0)	0.22[e]	650	0.36	2.32	5.90	0.38	0.35	0.27	2.54	1.05
Por+cya (pH 7.4)	0.27[f]	650	0.31	2.36	5.61	0.22	0.38	0.4	3.21	1.14
In thin film studies										
$DiOC_6(3)$	—	550	0.19	0.48	2.69	0.74	0.24	0.02	0.31	1.14
H_4TPPS^{2-}	—	660	0.30	1.16	4.74	0.68	0.25	0.07	0.83	1.13
H_2TPPS^{4-}	—	670	0.24	0.61	2.77	0.76	0.23	0.01	0.35	1.2
Por+cya (pH 3.0)	—	650	0.42	2.06	5.04	0.57	0.32	0.11	1.45	1.1
Por+cya (pH 7.4)	—	650	0.34	1.40	2.9	0.46	0.4	0.14	1.12	0.99

[a]Quantum yield of H_4TPPS^{2-} is taken as 1.0, all other values are relative to H_4TPPS^{2-}. [b]Por = porphyrin and cya = [$DiOC_6(3)$]. Also por : cya is in the ratio of 1 : 4. [c]λ_{ex} = 433 nm. [d]λ_{ex} = 413 nm. [e]λ_{ex} = 520 nm. [f]λ_{ex} = 520 nm.

dianion porphyrin H_4TPPS^{2-} is 3.85 ns and that of tetraanion H_2TPPS^{4-} is 9.26 ns. The decay for the aggregates was obtained in solution as well as thin film. The fluorescence decay of the porphyrin–cyanine aggregate in solution (colloidal suspension) or thin film was multiexponential and the results are tabulated in Table 1. Thin films of the porphyrin anions and cyanine were also measured and the fluorescence decay was multiexponential in each case (Table 1).

Resonance light scattering (RLS) and dynamic light scattering (DLS) studies

The porphyrin–cyanine aggregate described above is stable in solution at low total concentration (<10 μM). The nature of the aggregate in the solution was studied by resonance light scattering (RLS) and dynamic light scattering (DLS). Dynamic light scattering studies showed that the particle size varies from 200 nm to 800 nm. Fig. 7 shows the RLS spectra of H_4TPPS^{2-} (5 μM) in pH 3 that were obtained for different concentrations of $DiOC_6(3)$. The background RLS spectrum of the buffer is subtracted in each case. The RLS spectrum of colloidal aggregates reveals a Rayleigh scattering background superimposed with absorption (dip due to monomer absorption) and enhanced scattering (prominence at 540 nm). Curves a and b are the RLS spectra for the free porphyrin (5 μM) and free cyanine (20 μM) which show only dips at 433 nm and 480 nm, which are the absorption maxima of the two molecules, respectively. Curves c–f are the RLS spectra for porphyrin–cyanine solutions in the ratio of 1 : 1, 1 : 2, 1 : 3 and 1 : 4. The increased light scattering is observed even at a ratio of 1 : 1 (curve c). The dip in the RLS spectrum is observed only at 433 nm and not at 480 nm indicating that all the cyanine dye molecules are completely consumed in the formation of aggregates. Further, a scattering prominence is observed at 540 nm, which is the absorption edge of the porphyrin–cyanine aggregate. The scattering prominence is more enhanced at higher ratios (curves d–f) and a dip due to free dye absorption at 480 nm is indicated only at the ratio of 1 : 4.

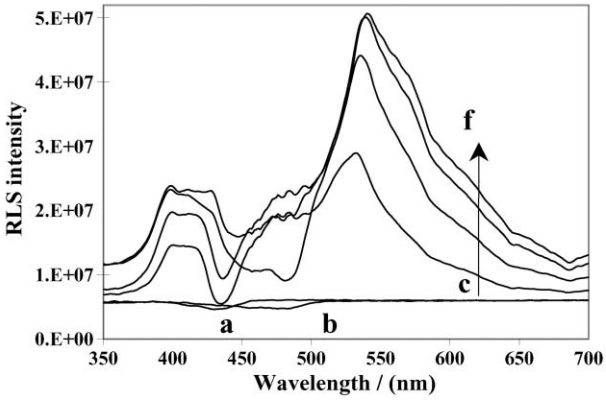

Fig. 7 Resonance light scattering (RLS) results. (a) RLS of H_4TPPS^{2-} (5 μM) in pH 3.0 buffer. (b) RLS of $DiOC_6(3)$ (5 μM) in pH 3.0 buffer. RLS of the cyanine-aggregate of H_4TPPS^{2-} (5 μM) and $DiOC_6(3)$ of concentration ratio 1 : 1 (c), of concentration ratio 1 : 2 (d), of concentration ratio 1 : 3 (e), and of concentration ratio 1 : 4 (f).

Circular dichroism

It is known that self-assembled molecular aggregates may exhibit spatial ordering and thus induced linear or circular dichroism,[25] particularly in porphyrin aggregates.[16] The aggregate that was formed by interaction of H_4TPPS^{2-} or H_2TPPS^{4-} and $DiOC_6(3)$ was found to be inactive in circular dichroism.

IV. Discussion

The strong interaction of negatively charged H_4TPPS^{2-} with H^+ in acid solutions,[31] or positively charged inorganic,[13] cationic porphyrin[29a] and cationic surfactant[14] have been reported earlier. In most of the cases, J-aggregation of the porphyrin was induced with varying degree of efficiency and a prominent J-band was observed at ~490 nm. Positively charged cyanine dyes are another class of dyes that are well known to form J-aggregates at a relatively high concentration and perhaps most extensively studied[3] and used in photographic applications. It is therefore interesting to study the nature of the molecular aggregate, if formed, by the electrostatic interaction between the negatively charged H_4TPPS^{2-} and positively charged cyanine dyes.

In this study, two cyanine dyes with ethyl and hexyl chains, $DiOC_2(3)$ and $DiOC_6(3)$ were used. The results described before (Fig. 2 and 3) shows that there is no interaction between H_4TPPS^{2-} and $DiOC_2(3)$ whereas H_4TPPS^{2-} and $DiOC_6(3)$ readily forms a molecular aggregate. The difference between the structures of cyanine dyes is in the length of the alkyl chains (Fig. 1), ethyl *vs.* hexyl, attached to the nitrogen. The electrostatic interaction being equal for both cyanines, the longer alkyl chain aids molecular aggregation.

In the case of $DiOC_6(3)$, molecular aggregation is efficient even at very low concentrations of porphyrin. This is indicated by the absence of absorbance due to the free dye in the absorption and RLS spectra when the porphyrin : cyanine ratio is 1 : 1. The dye is completely consumed in the formation of the aggregate for ratios up to 1 : 3. The new absorption bands (500–550 nm) that are observed in the aggregate suggest that there have been significant changes in the chemical structure of both porphyrin and the cyanine.

Structure of porphyrin and cyanine, and type of aggregate

The stoichiometry of porphyrin : cyanine in the aggregate was found to be 1 : 4. The porphyrin is a dianion and the cyanine is a monocation. The ratio 1 : 4 implies that the basic macromolecular assembly will carry a net positive charge of 2 units per assembly containing one porphyrin and four cyanine molecules. On the other hand, the porphyrin–cyanine molecular assembly readily aggregates to colloidal dimensions and eventually separates out from the solution. Organic macromolecules such as proteins tend to aggregate and precipitate under conditions when they are neutralized.[33] This suggests that the charge of the porphyrin–cyanine macromolecular assembly may be zero. This is possible only if the porphyrin–cyanine molecular assembly loses two protons from the porphyrin macrocycle in the process of aggregation. Spectroscopic evidence (see below) gives support to the theory that the structure of the porphyrin in the aggregate is similar to a tetraanion, H_2TPPS^{4-}. This is further supported by the formation of aggregate between cyanine and tetraanion with the same composition.

The Soret peak of the porphyrin dianion (pH 3) in the absorption spectrum appears at 433 nm whereas the Soret peak of the tetraanion (pH 7.4) appears at 412 nm. In the molecular aggregate of $DiOC_6(3)$ and H_4TPPS^{2-}, the Soret peak is red shifted (with respect to the tetraanion) to 420 nm. Similarly, the fluorescence emission of the aggregate shows two emission bands at 654 and 718 nm which are similar to the spectrum of the tetraanion (Fig. 6, peaks at 644 and 705 nm) rather than that of the dianion (single peak at 670 nm). Thus, the porphyrin in the molecular aggregate is a tetraanion, H_2TPPS^{4-}, with the loss of two protons from the macrocycle. That is, the porphyrin molecule is deprotonated even though the pH of the solution is 3. Such a deprotonation is possible only when the porphyrin molecule is shielded from the aqueous environment. The four cyanine molecules, aided by the eight hexyl chains may provide such a nonaqueous shield to the porphyrin macrocycle.

Deprotonation of the porphyrin macrocycle in the dianion H_4TPPS^{2-} occurs in aqueous micellar solution even at low pH.[14] In micelles, the porphyrin is intercalated into the micelle and thus a nonaqueous shield is available for the deprotonated molecule, shielding it from the high proton concentration in water. By analogy with the example of micelles, one may expect that in the macromolecular porphyrin–cyanine aggregate the porphyrin is shielded by a nonaqueous environment. An important difference between the micelle–porphyrin aggregate and the cyanine–porphyrin aggregate is that in the former case, there is only one porphyrin per aggregate, which resembles closely the spectroscopic properties of the tetraanion. In the case of the porphyrin–cyanine aggregate, there are many porphyrin molecules per aggregate. The spectroscopic and fluorescence decay properties of the aggregate are therefore different from those of the monomer tetraanion.

The fluorescence spectrum of the cyanine–porphyrin aggregate is similar to that of the tetraanion, but the peak is red-shifted by 12 nm compared to the tetraanion in water. Another difference is that the spectrum is narrow compared to the monomer. Narrowing of the spectrum of the dye in aggregates is associated with an ordered arrangement of the chromophores.[34] The two possible ordered arrangements of the dye molecules are called H-aggregate (molecules stacked like a pack of cards) and J-aggregate (side-by-side arrangement of molecules).[8] The transition moments of the molecules are coupled in such ordered arrangements and the absorption and emission spectra become narrow. The spectral width (in cm^{-1}) of the aggregate is less than that of the monomer by $N^{1/2}$, where N is the number of molecules that are electronically coupled in the 'ordered' arrangement.[34,35] N is the spectroscopic aggregation number, which is different from the number of dye molecules in the colloidal or particulate aggregate that may be very large. In the case of the porphyrin–cyanine aggregate, the fluorescence emission bandwidth is 556 cm^{-1} compared to that of the monomer which is 878 cm^{-1} (Fig. 6). The spectroscopic aggregation number of the porphyrin in the aggregate is calculated to be 2.5. This dimer-like porphyrin aggregate is inferred to be J-type because its absorption peak at 420 nm is red shifted with respect to tetraanion peak at 412 nm.

Coming to the cyanine dye molecule, the spectroscopic data suggest that its structure in the porphyrin–cyanine aggregate is different from the free dye molecule in the buffer at pH 3. The absorption band at 484 nm seen for the free dye is barely observed in the aggregate. Instead, a broad structureless band extending from 450–550 nm is observed. Our study of pH dependence of the absorption spectrum of the cyanine dye showed that its absorption spectrum is unchanged in the range, $1 < pH < 10$. Thus, the red shifted broad absorption band in the aggregate cannot be interpreted as a protonation effect on the cyanine dye, even though the porphyrin has been deprotonated in the same aggregate. The fact that cyanine and porphyrin are quantitatively recovered in their original state by dissolving the aggregate film in methanol rules out chemical mechanisms like permanent bond formation. Charge transfer in the ground state can also be ruled out because of the high values of redox potential of the cyanine[36] and porphyrin.[37] The only physical mechanism that can reasonably explain the red shifted band of cyanine at 500–550 nm is the aggregation effect on the electronic transition of the cyanine dye.

Resonance light scattering of the molecular aggregate indicates a prominence at 540 nm (Fig. 7). Such a prominence indicates a resonance effect on the scattering intensity due to electronic absorption, which is observable only in aggregates of chromophores. The RLS intensity is proportional to the sum of the squares of the real and imaginary parts of the complex index of refraction.[15] The real part of the refractive index varies slowly with wavelength; the imaginary part (due to absorption) varies sharply with wavelength. Thus, resonance enhancement of light scattering occurs in the region where the molecule absorbs intensely. Conversely, prominences in the RLS spectra may be attributed to chromophore aggregates with intense absorption. It was shown that J- and H-aggregates give RLS spectra that are relatively sharp and unambiguous.[15]

In the case of porphyrin–cyanine aggregate described here, the RLS spectrum shows an unambiguous prominence at 540 nm (Fig. 7). As discussed before, the absorption in this region is due to aggregates of the cyanine dye but there is no order in the arrangement of molecules that may be characterized as perfect J-type. Even though the RLS spectrum shows a prominence at 540 nm, the absorption spectrum of the aggregate itself does not show any prominent band at 540 nm (Fig. 3). This can be understood as an effect of several factors on which scattering intensity depends, namely, size and shape of the colloidal particles (which are distributed), coefficient of refractive index with concentration, and transition moment of the aggregate *vis-à-vis* the monomer.

Dynamic light scattering studies showed a unimodal distribution of particle sizes and the peak position and width are highly sensitive to the concentration and age of the sample. Typically, the size distribution is between 200 nm and 800 nm in early times and the aggregates precipitate or settle on the sides with time. Though the spectral narrowing of fluorescence emission shows only 2.5 molecules of porphyrin as spectroscopic aggregation, it is evident from DLS studies that the physical size of the aggregate is much larger and this can only be explained by the formation of larger structures from the individual small aggregates. The formation of larger structures may be due to the interaction of hydrophobic side chains of the cyanines in the individual aggregates.

Fluorescence decay of the aggregate

The characteristics of the fluorescence decay of the molecules and aggregates in solution and in thin film are useful to understand the photophysics of the porphyrin in the aggregate. The fluorescence decay of the porphyrin is single exponential both at pH 3 (dianion) and pH 7.4 (tetraanion) (see Table 1). The decay of the porphyrin becomes multiexponential in thin film, which is the result of self-quenching and other solid-state effects. The average lifetime in the thin film is very much less than that in the solution. The fluorescence decay of the porphyrin–cyanine aggregate is multiexponential in solution as well as the thin film. The three lifetimes ($\sim$0.4, 2.3 and 5.6 ns) are similar in pH 3 and pH 7.4 solutions but the amplitudes are different resulting in different average lifetimes. The short lifetime observed in the thin film of the aggregate is similar to that observed in solution, but the other two lifetimes are shorter and different in the two films, which can be explained by self-quenching. The spectroscopic results discussed before indicated that the nature of the porphyrin in the aggregation is tetraanion-like. The results of analysis of fluorescence decay are therefore consistent with the spectroscopic results.

The role of the hexyl chain in stabilizing the aggregate

The cyanines $DiOC_2(3)$ and $DiOC_6(3)$ differ in their structure by their side chains (Fig. 1). The fact that $DiOC_6(3)$, but not $DiOC_2(3)$, forms an aggregate with porphyrin leads to the conclusion that the hexyl chain in the cyanine $DiOC_6(3)$ is involved in stabilizing the aggregate formation. The interaction of the dye with the porphyrin is so strong that the dianion is even deprotonated in the aggregate in highly acidic solutions of pH 3 or 2. The ethyl chain in the cyanine, $DiOC_2(3)$ is too small for stabilizing the aggregate.

V. Conclusions

The interaction of anionic *meso*-tetrakis(4-sulfonatophenyl)-porphine (H_4TPPS^{2-} and H_2TPPS^{4-}) was studied with two cationic cyanines $DiOC_2(3)$ and $DiOC_6(3)$. Both the porphyrin anions form stable aggregates with the cyanine dye having hexyl side chains, $DiOC_6(3)$. The porphyrin : cyanine ratio in the aggregate is 1 : 4. UV–Vis, fluorescence, fluorescence lifetime and light scattering results were used to characterize the structure of porphyrin and cyanine in the aggregate. The cyanine dye, $DiOC_2(3)$, having ethyl chains does not form an aggregate with the porphyrin.

Acknowledgement

A. S. R. Koti acknowledges partial support from the Kanwal Rekhi Career Development Scholarship of the TIFR Endowment Fund.

References

1 J.-M. Lehn, *Supramolecular Chemistry: Concepts and Perspectives*, VCH, Weinheim, 1995.
2 M. Y. Okamura, G. Feher and N. Nelson, *Photosynthesis*, ed. Govindjee, Academic Press, New York, 1982, pp. 195–272.
3 T. Kobayashi, *J-Aggregates*, World Scientific, Singapore, 1996.
4 E. E. Jelly, *Nature (London)*, 1936, **138**, 1009.
5 G. Scheibe, *Angew. Chem.*, 1936, **49**, 563.
6 A. S. Davydov, *Theory of Molecular Excitons*, Plenum Press, New York, 1971.
7 F. C. Spano and S. Mukamel, *Phys. Rev. A*, 1989, **40**, 5783.
8 P. W. Bohn, *Annu. Rev. Phys. Chem.*, 1993, **44**, 37.
9 V. Czikklely, H. D. Forsterling and H. Kuhn, *Chem. Phys. Lett.*, 1970, **6**, 207.
10 F. Nuesch and M. Gratzel, *Chem. Phys.*, 1995, **193**, 1.
11 R. F. Pasternack, P. R. Huber, P. Boyd, G. Engasser, L. Francesconi, E. Gibbs, P. Fasella, G. C. Venturo and L. D. Hinds, *J. Am. Chem. Soc.*, 1972, **94**, 4511.
12 N. C. Maiti, M. Ravikanth, S. Mazumdar and N. Periasamy, *J. Phys. Chem.*, 1995, **99**, 17192.
13 N. C. Maiti, S. Mazumdar and N. Periasamy, *Curr. Sci.*, 1996, **70**, 997.
14 N. C. Maiti, S. Mazumdar and N. Periasamy, *J. Phys. Chem. B*, 1998, **102**, 1528.
15 R. F. Pasternack and P. J. Collings, *Science*, 1995, **269**, 935.
16 O. Ohno, Y. Kaizu and H. Kobayashi, *J. Chem. Phys.*, 1993, **99**, 4128.
17 F. Mallamace, N. Micali, S. Trusso, L. M. Scolaro, A. Romeo, A. Terracina and R. F. Pasternack, *Phys. Rev. Lett.*, 1996, **76**, 4741.
18 W. West and P. B. Gilman, in *Theory of the Photographic Process*, ed. T. H. James, Macmillan, New York, 1977.
19 P. F. Fahey, D. E. Koppel, L. S. Barak, D. E. Wolf, E. L. Elson and W. W. Webb, *Science*, 1977, **195**, 305.
20 Z. Derzko and K. Jacobson, *Biochemistry*, 1980, **19**, 6050.
21 B. A. Armitage and D. F. O'Brien, *J. Am. Chem. Soc.*, 1992, **114**, 7396.
22 P. R. Dragsten and W. W. Webb, *Biochemistry*, 1978, **17**, 5228.
23 M. Reers, T. W. Smith and L. B. Chen, *Biochemistry*, 1991, **30**, 4480.
24 J. L. Seifert, R. E. Connor, S. A. Kushon, M. Wang and B. A. Armitage, *J. Am. Chem. Soc.*, 1999, **121**, 2987.
25 M. Wang, G. L. Silva and B. A. Armitage, *J. Am. Chem. Soc.*, 2000, **122**, 9977.
26 E. J. Gibbs, I. Tinoco Jr., M. F. Maestre, P. A. Ellinas and R. F. Pasternack, *Biochem. Biophys. Res. Commun.*, 1988, **157**, 350.
27 T. M. Cooper and M. O. Stone, *Langmuir*, 1998, **14**, 6662.
28 N. Nakashima and T. Kunitake, *J. Am. Chem. Soc.*, 1982, **104**, 4261.
29 (*a*) E. Ojadi, R. Selzer and H. Linschitz, *J. Am. Chem. Soc.*, 1985, **107**, 7783; (*b*) U. Hofstra, R. B. M. Koehorst and T. J. Schaafsma, *Chem. Phys. Lett.*, 1986, **130**, 555; (*c*) C. Endisch, J.–H. Fuhrhop, J. Buschmann, P. Luger and U. Siggel, *J. Am. Chem. Soc.*, 1996, **118**, 6671.
30 R. P. Haugland, *Handbook of Fluorescence Probes and Research Chemicals*, Sixth Edition, Molecular Probes, Inc., Eugene, Oregon, USA, 1996.
31 E. B. Fleischer, J. M. Palmer, T. S. Srivastava and A. Chatterjee, *J. Am. Chem. Soc.*, 1971, **93**, 3162.
32 N. Periasamy, G. B. Maiya, S. Doraiswamy and B. Venkataraman, *J. Chem. Phys.*, 1988, **88**, 1638.
33 C. Tanford, *The Hydrophobic Effect: Formation of Micelles and Biological Membranes*, Wiley-Interscience, Canada, 1980.
34 E. W. Knapp, *Chem. Phys. Lett.*, 1984, **85**, 73.
35 E. W. Knapp, P. O. Scherer and S. F. Fischer, *Chem. Phys. Lett.*, 1984, **111**, 481.
36 T. Tani, K. Ohzeki and K. Seki, *J. Electrochem. Soc.*, 1991, **138**, 1411.
37 R. H. Felton, *The Porphyrins, Vol. V*, ed. D. Dolphin, Academic Press, New York, 1978, pp. 53–125.